Electronic supplementary material

# Loss in the making: absence of pelvic fins and paedomorphic pelvic girdles in a Late Devonian antiarch placoderm (jawed stem-gnathostome)

France Charest [1, 2], Zerina Johanson [3] and Richard Cloutier [1]

[1.] Université du Québec à Rimouski, Rimouski, Québec, Canada G5L 3A1

[2.] Parc national de Miguasha, Nouvelle, Québec, Canada G0C 2E0

[3.] Natural History Museum, London, United Kingdom SW7 5BD

* Corresponding author: richard_cloutier@uqar.ca

## Supplementary materials and methods

### Notes on the size series of *Bothriolepis canadensis*

The extensive size series composed of more than 340 specimens ranging from 4 to 205 mm in total dorsal armour length is housed in the collections of the MHNM. Most specimens ranging from 4 to 13 mm are from an exceptional assemblage corresponding to a fish nursery, or an effective juvenile habitat [23]. Data on the smallest specimens of this series will be covered in future publications, since the girdles were likely not developed in these very small larval(?) to juvenile specimens.

### Notes on the preparation of the pelvic area in *Bothriolepis*

The *Bothriolepis* pelvic girdle could easily go unnoticed and partial rotation of the girdle suggests that it could be easily displaced, or lost after decay (e.g., main text figure 1*g*; table S1). For example, two girdles were found alone, disarticulated from the specimen (MHNM 02-4263; MHNM 06-1688a), while in Johanson and Trinajstic ([24], figure 1A), the *Bothriolepis* specimen NHMUK PV P.6777 shows a pelvic girdle that is displaced to the left. When the pelvic area is carefully prepared specifically for the pelvic girdle, it is present in most specimens, but one has to be careful since the girdle could easily be detached from the specimen during the removal of the sediment. Thus, the small number of specimens showing the pelvic girdle (32) versus the large number of specimens examined here (340) should not be considered as the actual frequency of the pelvic girdle in *Bothriolepis canadensis*.

**Notes on the statistical approach for allometric growth**

Allometric growth was estimate on two pairs of variable, Lpelg-TALd and Wpelg-TALd, with the confidence intervals of the slope from the major axis (MA) and two ordinary least-square regressions (OLS; [25]) on $\log_{10}$ data, to obtain linear bivariate relationships and follow the test assumptions. The use of MA and OLS (x-y and y-x) linear regressions allows considering the respective strengths and weaknesses of the two regression methods [26-29]. The hypothesis of isometry ($H_0$) is rejected when the confidence intervals of the three slopes exclude the theoretical value of 1 (isometry). Linear regression assumptions were verified; the pair of variables Wpelg-Lpelg does not meet the assumptions of bivariate normality (library MVN: Royston, Mardia and Henze–Zirkler tests) and equality of the error variances (heteroscedasticity; [28]; library car, score test for non-constant error variance), and thus it was not computed.

## Supplementary results

**Presence of scales in *Bothriolepis canadensis***

*Bothriolepis canadensis* is known for its absence of scales [21]. However, a few ovoid, 0.5-1-mm scales with 2-6 concentric lines and a central visceral pit (figures 2*b*-*c* and S1) were observed in the ventro-posterior part of the trunk in two specimens, one immature (MHNM 02-1454, 28.74-mm) and one medium-sized (MHNM 02-2864, 105.11-mm). In both specimens, these scales resemble the scales observed in juvenile specimens of the antiarch *Asterolepis ornata* [13]. This is another trait that could be considered paedomorphic in *B. canadensis*. Consequently, the "triradiate scales" mentioned by

Stensiö (1948, figure 56 in [6]) on the putative pelvic fins of *Bothriolepis canadensis* do not correspond to actual scales.

## Supplementary discussion

The addition of the only, mostly complete, specimen of the basal *Parayunnanolepis* [30] in the *Bothriolepis* ontogenetic trajectory of pelvic girdle length relative to TALd shows that for a given size, the pelvic girdle is proportionally smaller in *Bothriolepis* relative to *Parayunnanolepis*. However, comparative ontogenetic trajectories, of basal and derived taxa, are crucial to infer allometric growth patterns and heterochrony (allometric heterochrony [31,32]). There is ambiguity regarding the ontogenetic status of the holotype specimen of *Parayunnanolepis xitunensis* [30]. But, considering: (i) *Parayunnanolepis* is characterized by its small size [30], (ii) yunnanolepiforms are generally small or medium-size antiarchs [33], and (iii) the medioventral (MV) opening (MV plate not visible) seems small (figure 1*c* in [30]; figure 1*b* in [3]) as in other small-sized yunnanolepids (e.g., *Yunnanolepis porifera,* fig. 7 in [34]), whereas a large ventral opening is recognized as an immature feature in antiarchs ([13,35,36]; except for the sinolepid antiarchs characterized by the absence of a MV plates and a large ventral opening [34,37]), the *Parayunnanolepis* specimen is likely an adult of a small species.

The *Bothriolepis* pelvic girdle represents 2.9% to 11% of TALd (table S2), whereas, the *Parayunnanolepis* girdle represents 9.5% of TALd (2.6-mm:27.35-mm). Consequently, there is not much difference in the relative size of the pelvic girdle between our largest mature *Bothriolepis* (9.6%; table S2) and *Parayunnanolepis*, but the importance of this difference depends on how mature it is compared with the largest

*Bothriolepis* of our sample, since in mature medium-sized (ca. 100-mm) *Bothriolepis* specimens the relative size of the pelvic girdle shows a lot of variation, from 6.3 to 10% of TALd. Thus, as noted, clear comparisons are not possible owing to the absence of a whole ontogenetic trajectory for *Parayunnanolepis*, crucial for inferring precise allometric heterochronic patterns in fossil species [31,32].

**First unambiguous ossified endoskeleton in antiarch placoderms**

In our description of the *Bothriolepis* pelvic girdle, we demonstrated for the first time in antiarchs a mineralized post-cranial endoskeleton made of: (i) perichondral bone, shared by jawless galeaspids, osteostracans and gnathostomes [38] but with an uncertain presence in antiarchs ([12], table S1), and (ii) endochondral bone, considered an osteichthyan (crown-group gnathostome) synapomorphy [38]. Incipient endochondral bone [38], appearing as small portions of trabecular bone within perichondrally-ossified endocranium, is documented in osteostracans and certain placoderms [39-43], and now also here between the perichondral bone layers in the *Bothriolepis* pelvic girdle. As well, resorption is present, with resorption being an important component in the pathway of endochondral bone development in osteichthyans (including tetrapods), removing the mineralized cartilage precursor to provide a scaffold for bone deposition.

Consequently, this provides additional support for the origin of endochondral bone at the agnathan-gnathostome transition, and representing an osteichthyan symplesiomorphy (inherited from stem-gnathostomes). Instead, it is the more extensive endochondral ossification that constitutes the osteichthyan synapomorphy. As well, presence of endochondral bone in basal jawed vertebrates such as antiarchs supports recent

hypotheses that chondrichthyans (sharks, rays, skates) share a loss of bone, rather than a primitive absence [44].

**Table S1.** Character coding relative to the presence or absence of perichondral bone for antiarch taxa in recent literature.

| Taxa | Coding | References |
|---|---|---|
| *Yunnanolepis* | Present | [4, 45, 46] |
| *Parayunnanolepis* | Unknown | [4, 11, 46, 47, 48] |
| | *Present* | [45] |
| *Sinolepis* | Unknown | [11, 46] |
| *Microbrachius* | Unknown | [4, 11, 46] |
| *Pterichthyodes* | Unknown | [4, 11, 46, 47, 48] |
| | *Absent* | [45, 49, 50] |
| *Remigolepis* | Absent | [11, 46] |
| | *Present* | [4] |
| *Bothriolepis* | Absent | [12, 45, 49, 50] |
| | *Present* | [4, 11, 46, 47, 48, 52] |

**Table S2.** Fossil specimens examined given in size order using total dorsal armor length (TALd). In some specimens, size is estimated using a proxy (indicated with an asterisk*); proxies are provided at the bottom of this table. Size of the pelvic girdle is described in terms of length (Lpelg) and width (Wpelg) of left (L) and right (R) half girdles, and relative proportion of LPelg relative to TALd (%TALd). Number of concentric lines (Conc. lines) are given for left and right girdles, when available. The length of fin radials (LRad) are given when these are observed. Specimens for which half girdle were found separated are identified. All measurements are given in millimeters (mm).

| Specimens | TALd | Proxy[1] | Lpelg[2] | | | Wpelg[2] | | Conc. lines[3] | | LRad | Girdles apart |
|---|---|---|---|---|---|---|---|---|---|---|---|
| | | | L | R | %TALd | L | R | L | R | | |
| MHNM 02-1454 | 28.74 | | 0.834 | NA | 2.9 | 1.146 | NA | 4 | - | 0.7 | |
| MHNM 02-3749 | 32.74 | | 1.480 | 1.347 | 4.3 | NA | 0.793 | - | 4 | - | |
| MHNM 02-3078 | 35.28 | | 1.546 | NA | 4.4 | 1.334 | NA | 11 | - | - | |
| MHNM 02-1421 | 39.93 | | NA | NA | NA | NA | NA | - | 8 | - | |
| MHNM 02-275 | 44.26 | | NA | NA | NA | NA | NA | - | 5 | - | |
| MHNM 02-3821 | 46.25 | | 1.863 | 1.695 | 3.8 | NA | 2.113 | 16 | - | - | |
| MHNM 02-1396 | 47.42* | b | NA | NA | NA | NA | NA | - | - | - | |
| MHNM 02-2426 | 48.69* | a | NA | NA | NA | 1.620 | NA | 9 | 9 | 1.07 | |
| MHNM 02-3170 | 57.25 | | NA | 2.368 | 4.1 | 2.276 | 2.396 | 14 | 14 | - | |
| MHNM 02-2848 | 57.96* | a | NA | NA | NA | NA | NA | - | - | - | |
| MHNM 02-446 | 61.42 | | 2.910 | 2.963 | 9.6 | 2.301 | 2.625 | 15 | 12 | - | |
| MHNM 02-3333 | 62.99 | | NA | NA | NA | 3.252 | 3.074 | 15 | 19 | - | |
| MHNM 02-3397 | 70.59 | | 2.960 | 2.934 | 4.2 | NA | 2.435 | 11 | 10 | - | X |
| MHNM 02-3412 | 79.94 | | 4.028 | 4.541 | 5.4 | 3.005 | 3.304 | 14 | 13 | - | |
| MHNM 02-3206 | 82.14* | a | 8.102 | 7.980 | 9.8 | NA | 5.586 | ? | 14 | - | |
| MHNM 02-988 | 83.97* | b | 4.566 | 4.510 | 5.4 | 4.409 | 4.456 | 21 | 24 | - | |
| MHNM 02-4263[4] | 83.21* | d | 5.174 | 5.363 | 6.33 | 4.650 | 4.147 | 12 | 9 | - | |
| MHNM 02-373 | 90.78* | a | 4.905 | 4.834 | 5.4 | NA | 3.812 | 14 | 14 | - | X |
| MHNM 02-3260 | 91.80* | b | 6.665 | 6.643 | 7.2 | 5.939 | 6.005 | 13 | 14 | - | |
| MHNM 02-3633 | 93.43 | | NA | NA | NA | NA | NA | - | - | - | X |
| MHNM 02-2119 | 94.04* | a | 10.370 | NA | 11.1 | NA | NA | - | - | - | X |
| MHNM 02-194 | 102.36* | a | 6.472 | NA | 6.3 | 5.219 | 5.264 | - | - | - | |
| MHNM 02-3668 | 102.89* | c | 10.256 | 10.703 | 10.2 | 6.822 | 7.027 | 18 | 17 | - | |
| MHNM 02-2864 | 105.11* | b | 9.162 | NA | 8.7 | 6.631 | 7.342 | NA | NA | - | |

| | | | | | | | | | | | |
|---|---|---|---|---|---|---|---|---|---|---|---|
| MHNM 02-2325 | 117.98* | a | NA | NA | NA | NA | NA | NA | NA | - | X |
| MHNM 02-3314 | 118.96* | b | 10.619 | 10.602 | 8.9 | NA | 5.344 | NA | NA | - | |
| MHNM 06-1688a[4] | 134.27* | d | 9.50 | 9.468 | 7.1 | 8.263 | 7.691 | 12 | - | - | |
| MHNM 02-4501 | 141.48 | d | 8.402 | 8.636 | 6.0 | NA | NA | NA | NA | - | |
| MHNM 02-3980 | 143.70 | | NA | NA | NA | NA | NA | NA | NA | - | X |
| NHMUK P. 6777 | 147.27 | | 6.914 | 7.089 | 4.7 | 4.498 | 4.611 | 13 | 13 | - | |
| MHNM 02-296 | 159.37* | a | NA | NA | NA | NA | NA | NA | NA | - | X |
| MHNM 02-3461 | 186.28 | | 17.040 | 18.738 | 9.6 | 11.458 | 11.701 | NA | NA | - | |
| **Mean** | 87.27 | - | 6.37 | 6.50 | 6.61 | 4.55 | 4.72 | - | | | - |

MHNM; Musée d'Histoire Naturelle de Miguasha (Miguasha, Canada)

NHMUK; Natural History Museum (London, UK)

NA; incomplete pelvic girdles not allowing length and/or width measurements

[1.] Proxies

a) LAMD, median length of anterior medio-dorsal plate; TALd = 3.20927 + 2.70313(LAMD); $R^2$ = 0.9938; n = 139

b) LAVL, length of anterior ventro-lateral plate; TALd = -1.55189 + 2.24163(LAVL); $R^2$ = 0.9904; n = 21

c) LPVL, length of posterior ventro-lateral plate; TALd = 0.83758 + 2.06249(LPVL); $R^2$ = 0.9927; n = 22

d) Total Wpelg, total width of pelvic girdle; TALd = 20.453 + 7.134(Total Wpelg); $R^2$ = 0.9059; n = 20

[2.] When total width (Wpelg) and length (Lpelg) were needed in statistical analyses:

Total Lpelg = mean(Lpelg-L + Lpelg-R), OR Total Lpelg = Lpelg of the half girdle available

Total Wpelg = Wpelg-L + Wpelg-R; OR Total Wpelg = 2(Wpelg of the half girdle available)

L and R, refer to left and right girdles.

[3.] Number of concentric lines: the higher value of the left and right data is used when estimating the relation between the number of lines and the size of specimens.

[4.] Pelvic girdle found alone in the sediment

**Table S3.** Results of one sample t-tests to evaluate the bilateral symmetry of left and right half-girdles.

| Variables | n | t | Mean | Mean CI (2.5%-97.5%) | *p* [1] |
|---|---|---|---|---|---|
| Length (L minus R) | 16 | -1.4642 | -0.166375 | -0.4085647 - 0.0758147 | 0.1638 [2] |
| Width (L minus R) | 12 | -0.093165 | -0.011167 | -0.2749759 - 0.2526426 | 0.9274 [3] |

[1.] A $p \leq 0.05$ is considered significant.

[2.] Type II error: 0.72

[3.] Type II error: 0.97

[2-3.] Sample sizes are small and the type II error is high, but the difference between Land R girdles is small and both confidence intervals include the 0 value.

CI, confidence interval

n, sample size

**Table S4.** Results for spearman rank correlations between the number of concentric lines (nbLines) on the surface of the pelvic girdles and a variable representing size of the specimen (dorsal armour lenght; TALd) or of the pelvic girdle (length and width).

| Variables | n | $r_s$ | $p$ [1] |
|---|---|---|---|
| nbLines - TALd | 20 | 0.538511 | 0.0143 |
| nbLines - girdle width | 18 | 0.488808 | 0.0395 |
| nbLines - girdle length | 16 | 0.375523 | 0.1518 |

[1] A $p \leq 0.05$ is considered significant.

n, sample size

$r_s$, Spearman rank correlation coefficient

**Table S5.** Carbon, calcium, phosphorus and fluorine contents (mean weight percentage, wt%), and calcium/phosphorus (Ca/P) ratios in dermal bone and pelvic elements for five specimens of *Bothriolepis canadensis*.

| Material | Carbon (wt%) | Calcium (wt%) | Phosphorus (wt%) | Ca/P ratio[1] | F (wt%)[2] |
|---|---|---|---|---|---|
| **MHNM 02-1454** (28.74 mm[3]) | | | | | |
| Pelvic girdle | 4.77 | 29.35 | 13.42 | 2.19 | 5.33 |
| Radial? | 6.53 | 23.77 | 12.16 | 1.95 | 7.30 |
| Scale | 4.60 | 30.64 | 11.89 | 2.58 | 4.11 |
| **MHNM 02-3749** (32.74 mm) | | | | | |
| Dermal bone | 21.60 | 12.42 | 7.47 | 1.66 | 9.08 |
| Pelvic girdle | 16.81 | 20.54 | 9.71 | 2.11 | 4.83 |
| **MHNM 02-2426** (48.69 mm) | | | | | |
| Dermal bone | 4.72 | 32.54 | 14.28 | 2.28 | 5.74 |
| Pelvic girdle | 60.05 | 6.90 | 0.61 | 11.31 | - |
| Radial? | 5.67 | 28.68 | 13.14 | 2.18 | 6.69 |
| **MHNM 02-3170** (57.25 mm) | | | | | |
| Dermal bone | 3.19 | 29.65 | 12.83 | 2.31 | 4.87 |
| Pelvic girdle | 8.16 | 26.76 | 9.87 | 2.71 | 1.97 |
| **MHNM 02-2864** (105.11 mm) | | | | | |
| Pelvic girdle | 15.28 | 17.22 | 8.34 | 2.06 | 4.85 |
| Scales | 9.57 | 22.63 | 11.21 | 2.02 | 5.26 |

[1.] Ca/P ratios are calculated from the mean Ca and P contents.

[2.] The bone signature of *B. canadensis* shows the frequent presence of a weak percentage of fluorine which is expected in regard to previous elemental composition analyses made on Escuminac fossil vertebrates [53].

[3.] Size corresponds to TALd

**Table S6.** Linear regressions on $\log_{10}$ data to evaluate the presence of allometric growth of the pelvic girdle length and width relative to the total dorsal armour length (TALd) in *Bothriolepis canadensis*.

| Regressions | Variables (x-y) | n | Intercept | Slope | Slope CI (2.5%-97.5%) | *p* [1] |
|---|---|---|---|---|---|---|
| MA | $L_{10}$TALd - $L_{10}$Wpelg | 22 | -1.837394 | 1.426335 | 1.205881 - 1.704422 | 0.001 |
| OLS | $L_{10}$TALd - $L_{10}$Wpelg | 22 | -1.619626 | 1.310434 | 1.085218 - 1.535650 | 0.001 |
| OLS | $L_{10}$Wpelg - $L_{10}$TALd | 22 | 1.312804 | 0.6718879 | 0.5564148 - 0.7873610 | 0.001 |
| MA | $L_{10}$TALd - $L_{10}$Lpelg | 23 | -2.513522 | 1.674336 | 1.432410 - 1.981740 | 0.001 |
| OLS | $L_{10}$TALd - $L_{10}$Lpelg | 23 | -2.248089 | 1.534751 | 1.287187 - 1.782314 | 0.001 |
| OLS | $L_{10}$Lpelg - $L_{10}$TALd | 23 | 1.513786 | 0.5784841 | 0.4851715 - 0.6717967 | 0.001 |

[1.] A $p \leq 0.05$ is considered significant; *p* is for the sign of the slope.

CI, Confidence interval

Lpelg, Length of pelvic girdle

n, sample size

MA, Major Axis

OLS, Ordinary least square regression

TALd, Total dorsal Armour Length

Wpelg, Width of pelvic girdle

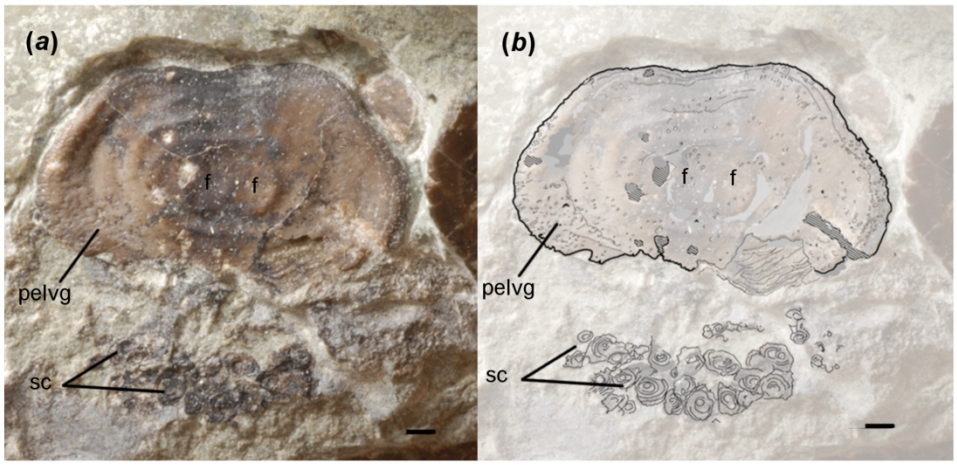


**Figure S1.** *Bothriolepis canadensis*, pelvic girdle. (*a*) Specimen MHNM 02-2864 shows a pelvic girdle (pelvg) with a relatively smooth surface and only few concentric lines, but with foci (f) still visible. Notably, a patch of scales (sc) is found just behind the pelvic girdle. (*b*) interpretive drawing. Scale bar: 1 mm.

## Supplementary references


23. Cloutier R. 2013 Great Canadian *Lagerstätten* 4. The Devonian Miguasha biota (Québec): UNESCO World Heritage site and a time capsule in the early history of vertebrates. *Geosci Can* **40**, 149-163. (doi: 10.12789/geocanj.2013.40.008).

24. Johanson Z, Trinajstic K. 2014 Fossilized ontogenies: the contribution of placoderm ontogeny to our understanding of the evolution of early gnathostomes. *Palaeont.* **57**, 505-516. (doi: 10.1111/pala.12093).

25. Cloutier R. 1997 Morphologie et variations du toit crânien du dipneuste *Scaumenacia curta* (Whiteaves) (Sarcopterygii), du Dévonien supérieur du Québec. *Geodiversitas* **19**, 61-105.

26. Smith RJ. 2009 Use and misuse of the reduced major axis for line-fitting. *Am. J. Phys. Anthropol.* **140**, 476–486. (doi: 10.1002/ajpa.21090).

27. Kilmer JT, Rodriguez RL. 2017 Ordinary least square regression is indicated for studies of allometry. *J. Evol. Biol*. **30,** 4-12. (doi: 10.1111/jeb.12986).

28. Legendre P., Legendre L. 1998 *Numerical Ecology*. Elsevier Science, Amsterdam.

29. Warton DI, Wright IJ, Falster DS, Westoby M. 2006 Bivariate line-fitting for allometry. *Biol. Rev.* **81**, 259–291. (doi: 10.1017/S1464793106007007).

30. Zhang G-R, Wang J-Q, Wang N-Z. 2001 The structure of pectoral fin and tail of Yunnanolepidoidei, with a discussion of the pectoral fin of chuchinolepids. *Vert. PalAsia.* **39,** 1-13.

31. McKinney ML, McNamara KJ. 1991 *Heterochrony: the evolution of ontogeny*. New York, Springer Science+Business Media.

32. Trinajstic K, McNamara KJ. 1999 Heterochrony in the Late Devonian arthrodiran fishes *Compagopiscis* and *Incisoscutum*. *Rec. West. Aust. Mus.* **57** (supp), 93-106.

33. Zhang, G-R, Wang S-T, Wang J-Q, Wang N-Z, Zhu M. 2010 A basal antiarch (placoderm fish) from the Silurian of Qujing, Yunnan, China. *Palaeoworld* **19**, 129-135. (doi: 10.1016/j.palwor.2009.11.006).

34. Zhu M. 1996 The phylogeny of the Antiarcha (Placodermi, Pisces), with the description of Early Devonian antiarchs from Qujing, Yunnan, China. *Bull. Mus. Natl. Hist. Nat.*, Paris, **18**, Section C, 233-347.

35. Young GC. 1988 Antiarchs (placoderm fishes) from the Devonian Aztec Siltstone, southern Victoria Land, Antartica. *Palaeont. Abt. A* **202**, 1-125.

36. Downs JP, Criswell KE, Daeschler EB. 2011 Mass mortality of juvenile antiarchs (*Bothriolepis* sp.) from the Catskill Formation (Upper Devonian, Famennian Stage), Tioga County, Pennsylvania. *Proc. Acad. Nat. Sci. Phila.* **161**, 191-203. (doi: 10.1635/053.161.0111).

37. Ritchie A, Wang S-T, Young GC, Zhang G. 1992 The Sinolepidae, a family of antiarchs (Placoderm fishes) from the Devonian of South China and Eastern Australia. *Rec. Aust. Mus.* **44**, 319-370.

38. Zhu M. 2014 Bone gain and loss: insights from genomes and fossils. *Natl. Sci. Rev.* **1**, 490–497. (doi: 10.1093/nsr/nwu062).

39. Wängsjö G. 1952 *The Downtonian and Devonian vertebrates of Spitsbergen. IX.* Norsk Polarinst. Skrift. **97**, 1–611.

40. Stensiö E. 1969 Arthrodires. In *Traité de Paléontologie* (ed J Piveteau), pp. 71–692. Paris, France: Masson et Cie.

41. Goujet D. 1984 Les poissons placodermes du Spitsberg: Arthrodires Dolichothoraci de la Formation de Wood Bay (Dévonien inférieur). *Cahiers de Paléontologie, Section Vertébrés* (Centre National de la Recherche Scientifique). 284 p.

42. Miles RS, Young GC. 1977 Placoderm interrelationships reconsidered in the light of new ptyctodontids from Gogo, Western Australia. In *Problems in Vertebrate Evolution* (eds SM Andrews, RS Miles, AD Walker), pp. 123–198. London: Academic press.

43. Ørvig T. 1951 Histologic studies of placoderms and fossil elasmobranchs. *Ark. Zool* **2**, 321–454.

44. Ryll B, Sanchez S, Haitina T, Tafforeau P, Ahlberg PE. 2014 The genome of *Callorhinchus* and the fossil record: a new perspective on SCPP gene evolution in gnathostomes. *Evol. Dev.* **16**, 123-124. (doi: 10.1111/ede.12071 ).

45. Brazeau, MD, de Winter,V. 2015 The hyoid arch and braincase anatomy of *Acanthodes* support chondrichthyan affinity of 'acanthodians.' *Proc. R. Soc. Lond. B Biol. Sci.* **282**, 20152210. (doi: 10.1098/rspb.2015.2210).

46. Qiao T, King B, Long JA, Ahlberg PE, Zhu M. 2016 Early gnathostome phylogeny revisited: Multiple Method Consensus. *PLoS ONE* **11**, e0163157. (doi: 10.1371/journal.pone.0163157).

47. Zhu, M. et al. 2013 A Silurian placoderm with osteichthyan-like marginal jaw bones. *Nature* **502**, 188–193. (doi:10.1038/nature12617).

48. Dupret V, Sanchez S, Goujet D, Tafforeau P, Ahlberg PE. 2014 A primitive placoderm sheds light on the origin of the jawed vertebrate face. *Nature* **507**, 500–503. (doi: 10.1038/nature12980).

49. Davis SP, Finarelli JA, Coates MI. 2012 *Acanthodes* and shark-like conditions in the last common ancestor of modern gnathostomes. *Nature* **486**, 247–250. (doi:10.1038/nature11080).

50. Brazeau, MD. 2009 The braincase and jaws of a Devonian "acanthodian" and modern gnathostome origins. *Nature* **457**, 305–308. (doi: 10.1038/nature07436).

51. Giles S, Rücklin M, Donoghue PCJ. 2013 Histology of "placoderm" dermal skeletons: Implications for the nature of the ancestral gnathostome. *J. Morphol.* **274**, 627–644. (doi: 10.1002/jmor.20119).

52. Young, G.C. 1984 Reconstruction of the jaws and braincase in the Devonian placoderm fish *Bothriolepis*. *Palaeont.* **27**, 635–661.

53. Chevrinais M, Balan E., Cloutier R. 2016 New insights in the ontogeny and taphonomy of the Devonian acanthodian *Triazeugacanthus affinis* from the Miguasha *Fossil-Lagerstätte*, eastern Canada. *Minerals* **6**. (doi:10.3390/min6010001).